FIGURE 10
The angle between the scanning directions in the SAR data used in the study

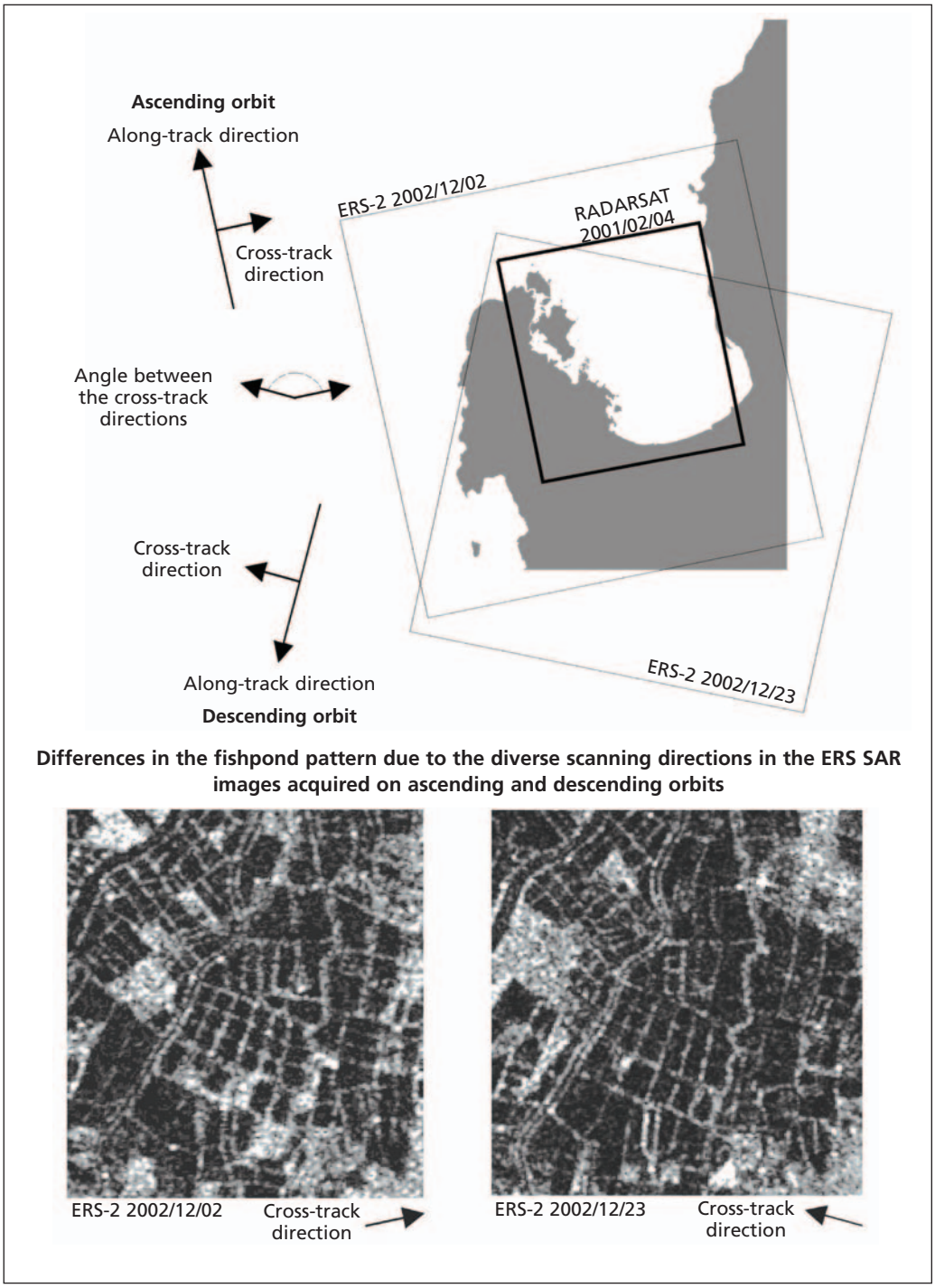

The other aquaculture and fisheries structures influence the radar signal in a similar way. The vertical sides of fish cages, pens and traps, emerging from the water surface, create the corner reflector effect that allows to identify them. For example, Figure 11 shows the interaction of SAR pulses with a fish cage. The sides of the cage oriented perpendicularly to the scanning direction are brighter in the SAR image.

In the smaller cages, the extension of the water surface inside is very small with respect to the sensor resolution and may not be represented in the image. As a result, the cage will appear as a bright group of pixels on the dark sea surface (Figure 12). The same happens to the smaller fish pens.

Both ERS and RADARSAT SAR sensors operate in the C-band (frequency 5.3 GHz, wavelength 5.6 cm). A SAR system generally sends out either horizontally (H) or vertically (V) polarized pulses, and collects either horizontally or vertically polarized return signals. The ERS SAR sends and receives vertically polarized signals (VV), while RADARSAT SAR sends and receives horizontally polarized signals (HH). Thus, both these sensors measure the portion of the backscattered signal which has maintained the original polarization.

FIGURE 11
Interactions of radar beams with a fish cage

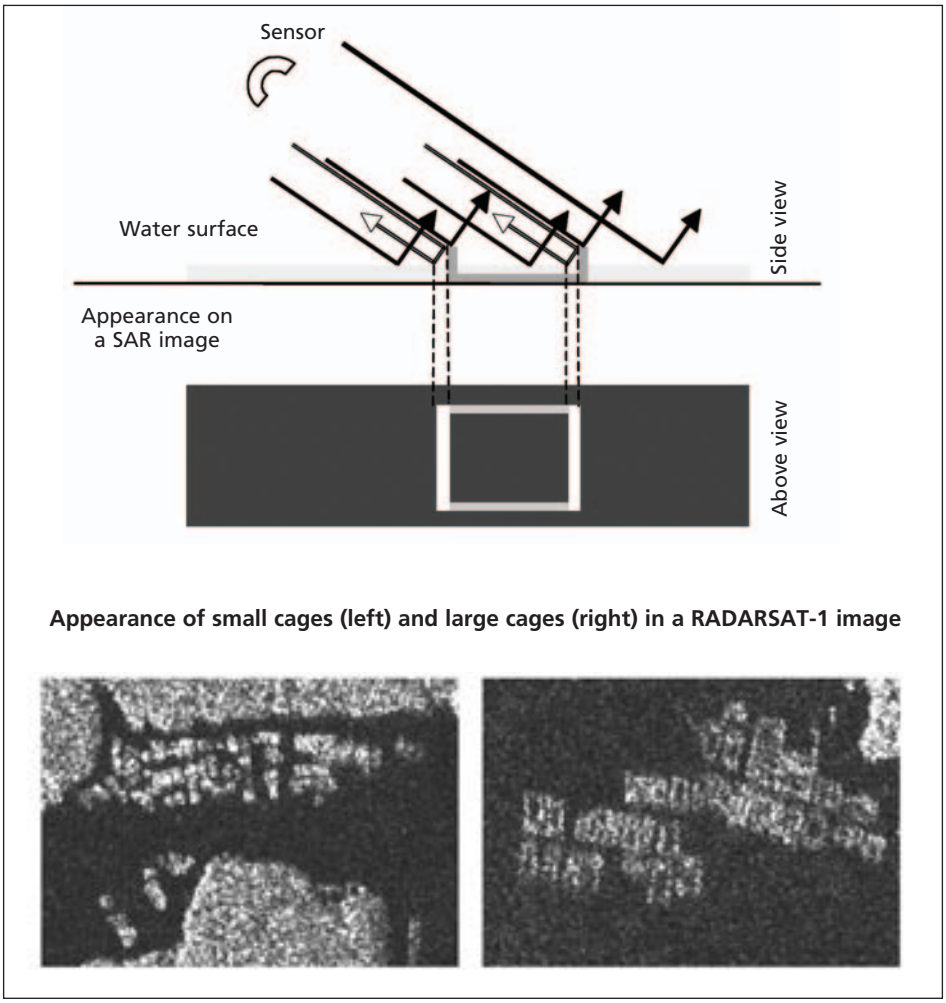

The differences in the appearance of various coastal land features, including fishponds, on ERS and RADARSAT imagery were studied by Paringit *et al.* (1998) on the area of the Panay-Guimaras Strait (the Philippines) using the airborne NASA/JPL AirSAR polarimetric system. Their results show that the mean backscattering coefficient of fishponds is slightly higher on C-band images acquired in VV polarization than in HH. VV data are, however, more sensitive to sea surface roughness (Touzi, 1999) which in turn depends on wind speed. Wind speeds greater than approximately 1.5 m/s (Fingas and Brown, 2000) create waves that increase the return signal intensity in C-band, diminishing the contrast among sea surface and the structures located offshore. The contrast keeps diminishing as the wind speed becomes more intense. This effect is clearly shown in Figure 12.

Fish cages are evident in the RADARSAT-1 image and in the first ERS image (of 2 December 2002); they are barely visible in the second ERS image (of 23 December 2002) due to the increased sea surface roughness. It should be noted that in the second ERS

image the coastline appears different, as the image was acquired during the receding tide; the emerging coral reefs contribute to increase sea surface roughness, thus reducing the possibilities of detecting fisheries structures.

Finally, the appearance of the structures in the SAR imagery is also greatly influenced by the spatial resolution of the sensor. Fisheries structures are generally made out of thin components and cover limited extensions; thus, the highest the spatial resolution the higher the possibility of detecting them. In particular, the smaller fish pens may not be evident in ERS SAR images, and fish traps are generally too thin to be detected; they appear only in the higher-resolution RADARSAT image (Figure 12).

FIGURE 12
Sea state and coastal aquaculture and fisheries structures mapping

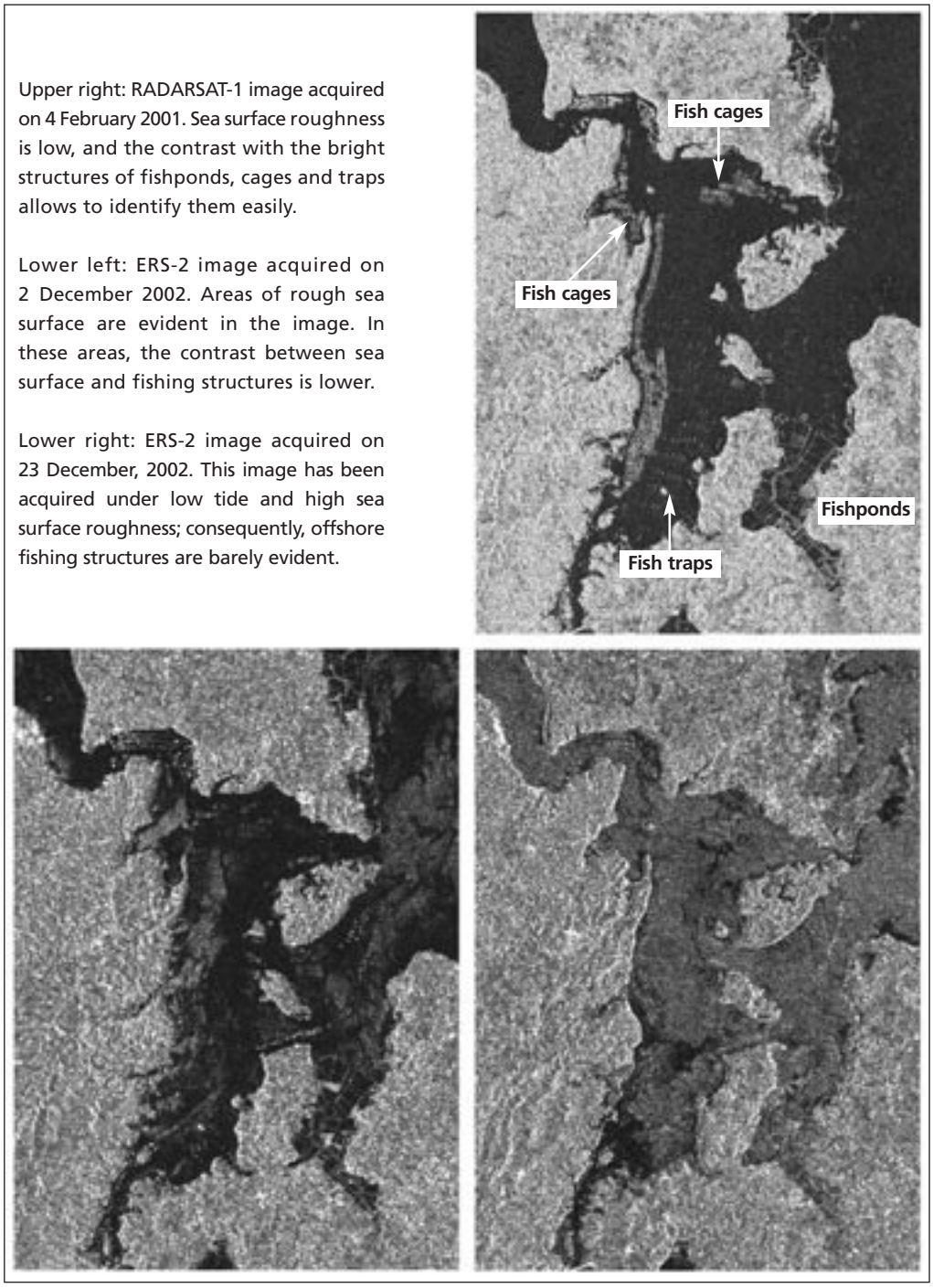

The visual interpretation procedures used to map coastal aquaculture and fisheries structures are described in section 2.6.

2.4 IMAGE PRE-PROCESSING PROCEDURE

In order to perform the visual interpretation of the SAR images, they must all be geocoded in the same projection of the reference cartography. Speckle-reducing filters also were applied to the images to verify whether it was possible to enhance their interpretability.

The SAR images were provided already geocoded: the ERS-2 projected into UTM/WGS 84, and the RADARSAT-1 into geographic/WGS72, as described in section 2.1. The reference cartography was represented into geographic/Clarke 1866, thus all the images were reprojected into geographic/Clarke 1866 so that they could be overlaid with one another and with the cartography.

The automatic reprojection procedures provided by the Erdas IMAGINE software were applied at first, but when the images generated by these procedures were overlaid on the cartography they showed consistent misplacements. It has thus been necessary to manually geocode each image, using the "non-linear rubber sheeting" procedure. This method is based on the identification, over the image and over the cartography, of a large number of ground control points (GCPs). The coordinates of each pixel on the new geocoded image are then obtained interpolating nonlinearly the coordinates of the surrounding reference points. All the three SAR images were geocoded using more than four hundred GCPs, reaching a RMS error lower than 1.5 pixels; the output pixel size is 0.00005825 decimal degrees, equivalent to 6.25 m.

SAR images are affected by the presence of noise (speckle), created by constructive and destructive interference between the backscattered energy from different portions of the ground surface included in the same pixel of the SAR image. The value of the affected pixels is thus increased or decreased; the SAR image appears to be covered by randomly scattered bright and dark spots.

Thus, to complete the image preparation, it may be useful to apply speckle reducing procedures to the SAR images in order to increase their interpretability.

A simple, yet useful technique has been tested by Profeti, Travaglia and Carlà (2003) on multi-temporal SAR data to improve the visual interpretation of fish ponds. This technique enhances time-invariant spatial features and reduces speckle, without compromising the geometrical resolution of the images. This method allowed to obtain good results; however, it can be applied only on multiple images of the same area acquired by the same sensor in the same acquisition geometry, while in this study the two ERS-2 images were acquired in ascending and descending orbits; therefore, it is not applicable in this case.

The most common speckle removal procedures are based on adaptive spatial filtering based on local statistics. The filters analyse each pixel's contextual information and produce a new image in which the value of each pixel is obtained from the values of its neighbouring pixels in the original image. Regardless of the specific filtering technique, noise reduction is achieved at the expense of the geometric detail of the image. Several filters proposed in literature (Lee, 1980 and 1981; Frost *et al.*,1982; Li, 1988) were tested upon each type of fisheries structure to be identified in the image, to evaluate their effectiveness in improving the structures' visual appearance.

The analysis of the results shows that the original images are sharper and richer in details, very useful for visual interpretation purposes. Consequently, no speckle removal filters were applied.

2.5 DIGITALIZATION OF THE SHORELINE

Differences among the shoreline profile can be observed between the two ERS-2 images. On the first (acquired on 2 December 2002), the emerged land is wider than on the second (acquired on 23 December 2002) and part of the coral reef is also visible. The difference between land and water among the RADARSAT and the second ERS-2 image is small, and is probably more related to scale difference and geocoding than to tide stage.

At present, several different shoreline definitions are in use by various state and local authorities. The U.S. National Oceanic and Atmospheric Administration

(NOAA) has adopted as standard shoreline the approximate line where the average high tide, known as Mean High Water (MHW), intersects the coast. In our case, the Philippines topographic maps use the Mean Lower Low Water (MLLW).

As no information on tides was available for the study area, it has not been possible to acquire images in a determined tide stage. Thus, it was decided to delineate the coastline by visual interpretation, using the image in which the coastline was more evident. To decide which image was best suited to be the reference for shoreline mapping, the scientific literature on this subject was reviewed. The use of airborne and spaceborne SAR imagery to delineate land boundaries has been tested widely in the last years; for example, RADARSAT imagery has been used to map the coastline on behalf the Digital Marine Resource Mapping (DMRM) program, initiated by the Government of Indonesia in 1996 (Hesselmans *et al.*, 2000). A wider scientific research on the use of new technologies for shoreline mapping is being conducted by NOAA and the U.S. National Geodetic Survey on behalf the Coastal Mapping Program. It includes experiments on the use of satellite SAR imagery, whose results show that RADARSAT fine mode (HH) enables to map the coastline within 28 m and at 98 percent confidence level with respect to shoreline data produced using conventional photogrammetric processes (Tuell, Lucas and Graham, 1999). Other sources confirmed that HH imagery is better suited for shoreline mapping than VV imagery (although quadpol image data are considered to be the most suitable at all).

Therefore, the RADARSAT fine mode image has been used to map the coastline in the small portion of the study area it covers (Figure 2). The ERS-2 image acquired on 23 December 2002 has been used to complete the coastline at high tide, while the other ERS-2 SAR image (of 2 December 2002) has been used to map the low-tide boundary.

To map the low-tide coastline, the second ERS-2 image was overlaid with the land/sea boundary at high tide. Whenever the differences were wider than two pixels, they were mapped; this limit distance has been assumed sufficient for compensating geocoding errors and positioning errors related to the different scanning direction.

2.6 MAPPING PROCEDURES

The description of the appearance of aquaculture and fisheries structures in SAR images, outlined in the previous sections, was used in the visual interpretation of the images.

The visual interpretation was performed using the Arc View software, as it is more suited for on-screen digitizing of the boundaries of the features. Two vector layers were created in order to collect the polygons and polylines of the classes of interest. Their content is described respectively in Tables 4a and 4b.

Polygons and polylines were digitized in the cartographic reference projection of the Philippines (section 2.1).

TABLE 4a
Classes identified in the SAR images: Polygon layer

Class Name	Notes
Salt pans 2002	No apparent changes from the extension mapped in 1977
Fishponds 2001 and 2002	Identified both on RADARSAT-1 and on the two ERS images
Fishponds 2001 and 2002, uncertain	Identified on one image only, out of two or three (where available)
Fish pens 2001	Identified on RADARSAT-1 data
Fish pens, uncertain	No assignments to this class
Fish cages 2001	Identified on the RADARSAT-1 image
Fish cages 2001, uncertain	May be a small island or a rough patch in the sea surface
Fish cages 2002	Identified on the ERS-2 images
Fish cages 2002, uncertain	May be a small island or a rough patch in the sea surface
Areas with fish traps in the open sea 2001	Polygons drawn around the areas on which fish traps were detected, to have an approximate estimation of their extension
Areas with fish traps inside rivers 2001	
Mainland, high tide	Coastline at high tide, obtained from RADARSAT-1 (2001/02/04) and the ERS-2 image acquired on 2002/12/02
Islands (open sea)	Islands inside the major rivers are not included

For each element located in the images, the following parameters were calculated:
– Polygons: area (km^2) and perimeter (km);
– Polylines: length (km).

The global area or length of the elements in each class have then been calculated and compared with the available ground truth from the topographic maps. The results are described in Chapter 3.

TABLE 4b
Classes identified in the SAR images: Polyline layer

Class Name	Notes
Traps in the open sea	Each line has been drawn on the segments composing the arrow-like traps, if detectable. Their length is thus an underestimation of the real value
Traps inside rivers	
Mainland + reef, low tide	Dry land at low tide, added to the "Mainland, high tide" class; it may include portions of the reef. Obtained from the ERS-2 image of 2002/12/23. Note that the image allows to recognize the coastline only on certain portions of the study area; thus, this class' polygons do not represent a complete map